Reducing Propulsion Airframe Aeroacoustic Interactions with Uniquely Tailored Chevrons: 1. Isolated Nozzles

Vinod G. Mengle[*], Ronen Elkoby[†], Leon Brusniak[‡]
The Boeing Company, Seattle, WA 98124-2207

and

Russ H. Thomas[§]
NASA Langley Research Center, Hampton, VA, 23681-2199

The flow/acoustic environment surrounding an engine nozzle installed on an airplane, say, under the wing, is asymmetric due to the pylon, the wing and the interaction of the exhaust jet with flaps on the wing. However, the conventional chevrons, which are azimuthally uniform serrations on the nozzle lip, do not exploit the asymmetry due to these propulsion airframe aeroacoustic interactions to reduce jet noise. In this pioneering study we use this non-axisymmetry to our advantage and examine if the total jet-related noise radiated to the ground can be reduced by using different types of azimuthally varying chevrons (AVC) which vary the mixing around the nozzle periphery. Several scale models of the isolated nozzle, representative of high bypass ratio engine nozzles, were made with a pylon and azimuthally varying chevrons on both fan and core nozzles to enhance mixing at the top (near the pylon) with less mixing at the bottom (away from the pylon) or vice versa. Various combinations of fan and core AVC nozzles were systematically tested at typical take-off conditions inside a free jet wind-tunnel and, here, in Part 1 we analyze the acoustics results for the isolated nozzle with a pylon, with installation effects reported in Parts 2 and 3. Several interesting results are discovered: amongst the fan AVCs the top-enhanced mixing *T-fan* chevron nozzle is quieter in combination with any core AVC nozzle when compared to conventional chevrons; however, the bottom-mixing *B-fan* chevrons, as well as the core AVC nozzles, by themselves, are noisier. Further, the low-frequency source strengths in the jet plume, obtained via phased microphone arrays, also corroborate the far field sound, and for the T-fan chevrons such sources move further downstream than those for baseline or conventional chevron nozzles.

Nomenclature

AVC	=	azimuthally varying chevron
b	=	sideline distance of phased array from the nozzle centerline
b	=	baseline round (no chevron) nozzle
B	=	bottom-enhanced mixing chevron nozzle
BANDN	=	$1/3^{rd}$ octave band (o.b.) number = $10*\log(1/3^{rd}$ o.b. frequency)
D	=	nozzle diameter
f	=	frequency (hz)
HFL	=	high frequency lift
L	=	axial location of a source
LSAF	=	low speed aeroacoustic facility (at Boeing)
M_{wt}	=	wind-tunnel Mach number
NPR_c, NPR_f	=	nozzle pressure ratio of core (or primary) and fan (or secondary) stream, respectively

---

[*] Engineer/Scientist, Acoustics & Fluid Mechanics Dept., P.O. Box 3707, MC: 67-ML, Sr. AIAA Member.
[†] Engineer/Scientist, 787 Product Development Group, P.O. Box 3707, MC: OR-MM, AIAA Member.
[‡] Engineer/Scientist, Acoustics & Fluid Mechanics Dept., P.O. Box 3707, MC: 67-ML.
[§] Senior Research Engineer, Aeroacoustics Branch, MS 166, Sr. AIAA Member.

$OASPL$	=	overall sound pressure level (dB)
p_{amb}	=	ambient pressure
PAA	=	propulsion airframe aeroacoustics
R	=	radial distance of polar array of microphones from the core nozzle exit center
R	=	reference state-of-the-art chevron (azimuthally uniform)
RH	=	relative humidity (%)
SPL	=	sound pressure level (dB)
TTR	=	ratio of total temperature of core stream to that of fan stream
T	=	temperature
T	=	top-enhanced mixing chevron nozzle
x, y, z	=	Cartesian coordinate system (right handed) with x in the axial direction, y in the horizontal direction and z in the vertical direction, and origin at the core nozzle exit plane center

I. Introduction

CHEVRONS which are specific types of periodic serrations on nozzle lips, have been found to reduce jet noise of modern high bypass turbofan engines in the pioneering studies on separate-flow nozzles by Janardan et al[1] and internally-mixed nozzles by Mengle[2, 3]. These serrations are typically of triangular shape with slight immersions in either of the streams flowing around them to enhance the large-scale mixing downstream by generating streamwise vorticity; this reduces the potential core length which decreases the centerline velocity downstream of the potential core, and which in turn reduces the low frequency jet noise associated with large-scales near that axial location. In separate flow nozzles, such chevrons can be on the core nozzle or the fan nozzle or both, but their shapes and sizes, to the best of the authors' knowledge, are repeated around the periphery of the nozzles, that is, the conventional chevrons are azimuthally uniform.

However, the flow/acoustic environment surrounding the nozzles on which such chevrons are located is not necessarily axisymmetric or periodic. For example, for separate-flow nozzles installed under the wing (i) the pylons used for installation are on the top side of the nozzles – which produces a top-bottom asymmetry, (ii) the upwash near the wing's leading edge causes top-bottom asymmetry, (iii) the wing can reflect the noise radiating from the jet plume towards the ground, and (iv) the jet plume itself or the ambient flow it entrains can interact with downstream high-lift devices, like flaps or flaperons – this interaction is again asymmetric and can generate jet-flap interaction noise. Thus, there is an inherent top-bottom asymmetry in the way the jet plume interacts with its surroundings principally due to the way in which an engine is installed on the aircraft. In this paper we try to exploit this asymmetry to our benefit by uniquely tailoring the chevrons from top to bottom.
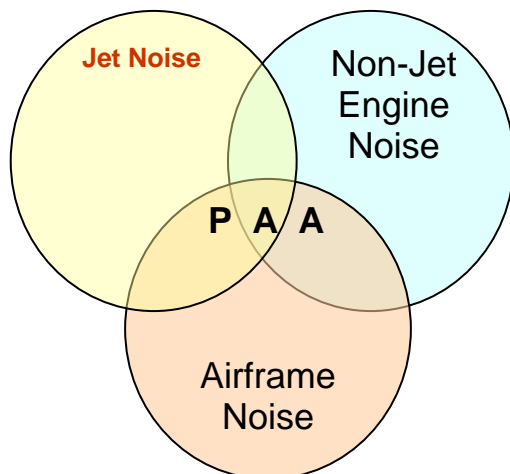

Figure 1. Venn diagram for Propulsion Airframe Aeroacoustic (PAA) interactions as an intersection of engine and airframe noise.

The interactions mentioned above are part of a nascent field of aeroacoustics called "Propulsion-Airframe Aeroacoustics (PAA)." These PAA interactions can be conveniently shown in a Venn diagram as the intersection of engine noise sources and airframe noise sources, as shown in Fig. 1. The engine has its own noise sources which can be conveniently categorized into jet noise sources, and non-jet noise sources, such as, fan noise, core noise, etc.; the airframe, on the other hand, has its own noise sources, such as, flap noise, slat noise, wing-tip noise, landing gear noise, etc. When the engine and the airframe are placed in each other's proximity, as is the practical case when the engine is installed under the wing, (i) these individual noise sources can be modified, (ii) new noise sources can be generated, like jet-flap interaction, or (iii) the manner in which noise travels from the source to the observer, or the propagation path, can be changed, say, due to reflection or diffraction from wings and flaps. All of these constitute PAA interactions.

This has spawned an additional area of research, namely, understanding of PAA installation effects for conventional chevron nozzles. PAA effects that are relevant include how the chevron nozzle might interact with or be impacted by the presence or integration with the pylon, the wing, and the flaps. The effect of the pylon on the development of the jet flow field and the resulting noise effects for conventional round nozzles has been studied, for example, at model scale by Bhat[4] and Hunter et al[5], and at full-scale by Elkoby[6]; whereas, more pertinent flow-acoustics work on pylon interaction in nozzles with conventional chevrons on the primary or core nozzle has been done at model scale by the NASA Langley PAA group[7, 8, 9]. These PAA studies indicate, for example, how core chevrons can change the flow-field downstream of the pylon both in the azimuthal and the axial direction, and hence change the far field noise characteristics.

With the background of these studies, the opportunity developed to take the highly successful chevron noise reduction approach and improve the overall jet-related noise reduction by accounting for the non-symmetric flow/acoustic interactions. In general, whenever there exists a source-observer acoustic asymmetry, as due to the PAA interactions mentioned above, it may be possible to radiate the noise away from the observer, effectively reducing it for the observer. Thus, for example, from community noise considerations where the observer is on the ground, as in take-off conditions, the aircraft noise, in particular, due to the exhaust jet can, perhaps, be radiated away from the ground observer by varying the mixing around the nozzle periphery in a certain manner. On the other hand, if the observer is in the fuselage, then the interior cabin noise, say, at cruise due to shockcells in the jet plume can, perhaps be radiated away from the fuselage by varying the mixing around the nozzle periphery in a different manner. This principle has led us to the concept of azimuthally varying chevrons (AVC) which is fully exploited here for the first time.

In order to understand each noise effect thoroughly we have divided the presentation of this work into several papers: noise from (1) isolated nozzles, inclusive of a pylon, (2) installed nozzles with a wing, including high-lift devices, and a fuselage, and (3) jet-flap interaction. This paper on isolated nozzles presents Part 1 of this series of three papers and the other two are being published simultaneously at this conference (Part 2[10] and Part 3[11]). This study was done as part of a broader Boeing and NASA partnership under the Quiet Technology Demonstrator 2 program which involved both model-scale tests and full-scale flight tests, as summarized in Herkes et al[12] .

In this paper, we introduce the concept of azimuthally varying chevrons (AVC) and experimentally study the case of AVC on realistic scaled isolated nozzles with a pylon. We systematically present the far field acoustic results for the case of individually varying the type of AVC on fan nozzle or the core nozzle or combinations of both with focus on community noise reduction at take-off conditions. Comparisons with state-of-the-art chevron nozzles and baseline simple splitter nozzles (without chevrons) are also shown. Finally, we also study the variations in the jet noise source strengths with different types of AVCs using phased arrays of microphones outside the free jet and examine if the source diagnostics results corroborate the far field acoustics results.

II.   Azimuthally Varying Chevron (AVC) Concept

As we mentioned earlier, the pylon is an essential part of a practical nozzle used for installation and gives an inherent top-bottom asymmetry: the outer fan flow is bifurcated due to it and the hot core flow grazes at its bottom. The flow near the pylon is fairly complex with two shear-layers (fan/ambient) on its sides, a hot core flow at its bottom and the pylon's own downstream wake. As mentioned earlier, several computational and experimental studies have been made by the NASA, Langley group[7,8,9] which capture the axial evolution of the olive-shaped or tear-drop asymmetry in the jet plume cross-section created due to the pylon and also the chevron/pylon interaction. In these studies[7,8,9], conventional chevrons appear to reduce the turbulence intensity downstream of the pylon in certain configurations. The idea proposed in this paper is that if we can further reduce the gradients in velocity and temperature near the pylon by even more vigorous enhanced-mixing on the fan nozzle then, perhaps, the strength of the turbulent eddies and entropic spots downstream of the pylon can be reduced even further, thus reducing the noise produced by them. Additionally, if these lower strength eddies interact with downstream bodies, like, flap trailing edges, etc., the noise produced due to their mutual interaction will also reduce the flap trailing edge noise[13] or the jet-flap interaction noise[14]. This interaction, however, depends on how the flap is located in relation to the jet plume – whether, it is only in the entrained flow outside the jet or inside it, and the situation is not completely clear.

Thus, the conventional azimuthally uniform chevrons, which enhance mixing compared to the baseline simple splitter nozzle (without chevrons), may also be able to reduce these sources of noise compared to the simple splitter nozzle. Such a regular chevron nozzle with similar chevron shape, size and immersions on both fan and core nozzle,

and simply referred to here as RR-nozzle[**], is shown in Figure 2(a). But now we would like to study the effect of additional enhanced mixing near the pylon at the top which can be achieved, for example, with chevrons of higher immersion and/or larger lengths. However, since high-frequency noise is known to increase with higher and higher immersion of chevrons[15], and the nozzle thrust and discharge coefficients tend to decrease, we may *not* want to immerse the chevrons around the whole periphery of the nozzle to the same higher value. Hence, the chevrons at the bottom, away from the pylon and the flaps, can be kept at lower immersions to compensate for these other deleterious effects. This leads to the idea of a nozzle with azimuthally varying chevrons (AVC) from top to bottom. Although there is a top-bottom asymmetry there is no particular reason for disturbing the left-right symmetry, at least for reduction of community noise when the ground observer also creates a top-bottom asymmetry.

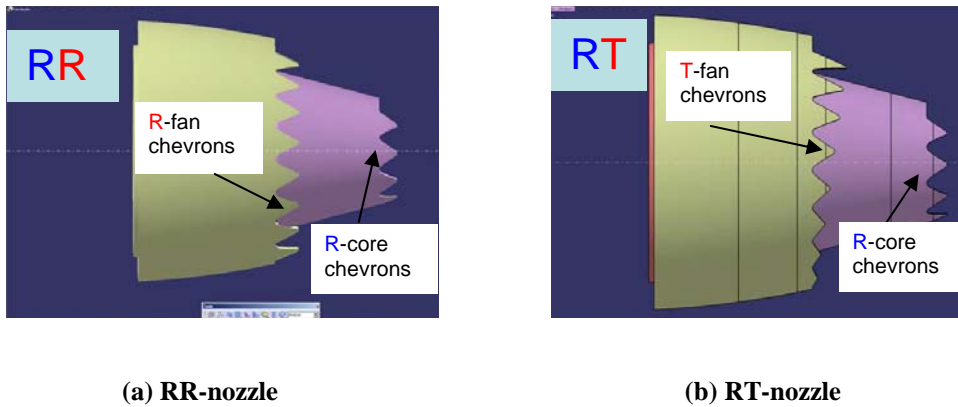**(a) RR-nozzle**   **(b) RT-nozzle**

Figure 2. Azimuthally varying chevrons (AVC) with top-enhanced mixing on fan nozzle (T-fan chevrons) in comparison to the regular (R) uniform chevrons: (a) RR-nozzle (b) RT-nozzle.

One embodiment of this AVC concept is, hence, the top-enhanced mixing chevrons (T-chevrons, for short) where the chevrons near the pylon (assumed to be on its top side) are bigger and more immersed compared to the chevrons away from the pylon (at the bottom) which are smaller and less immersed. Figure 2(b) shows one such T-fan chevron nozzle with a regular R-core chevron nozzle for comparison (hence, RT-nozzle). The azimuthal variation in mixing can be achieved by varying, for example, the chevron immersion or its length or both. Again, at this stage, we do not specifically prescribe any particular variation in mixing from top to bottom, such as, linear or non-linear, but the concept shown in Fig. 2(b) is a T-fan chevron nozzle with linear variation in chevron lengths and is one realization of this idea.

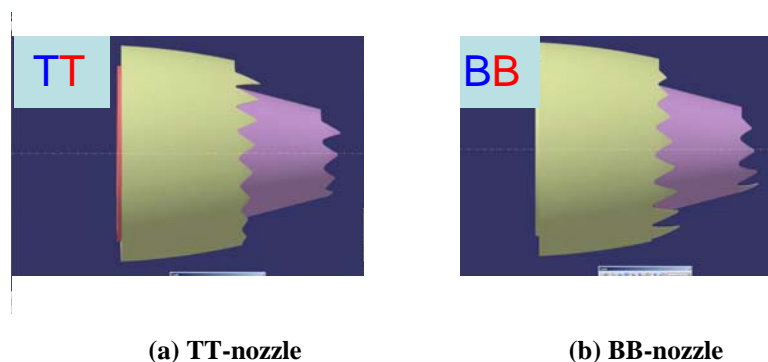**(a) TT-nozzle**   **(b) BB-nozzle**

Figure 3. Examples of combinations of different azimuthally varying chevrons (AVC) on core and fan nozzles (T = Top-enhanced mixing; B = Bottom-enhanced mixing): (a) TT-nozzle (b) BB-nozzle.

Now increased immersion is also known to increase turbulence kinetic energy and the high frequency spectrum, in general, (from several in-house studies at Boeing, or Bridges); hence, if such a source with high turbulence

---

[**] Here, we will use the notation R for regular or reference chevrons, and the notation XY-nozzle where X stands for the type of core nozzle and Y stands for the type of fan nozzle; hence, the nozzle shown in Fig. 2(a) is an RR-nozzle.

intensity is now closer to the wing (on the pylon side for the T-fan chevrons) then there is a possibility that there may be an increase in reflected noise of high frequency which may nullify any proposed advantage gained by the T-fan chevrons. It is also possible that due to enhanced mixing at the top, the shear-layer on the top has grown so wide that the downstream flap or flaperon which was previously outside the jet plume is now partially or completely bathed in it – this may increase the noise radiated from it rather than decreasing it. Hence, one also needs to examine the effects of enhancing the mixing at the bottom, away from the pylon, with less mixing at the top; one can use bottom-enhanced mixing chevrons (B-chevrons, for short) on the fan nozzle with larger and more immersed chevrons at the bottom (away from the pylon) compared to the smaller and less immersed chevrons at its top. The B-chevrons in this sense are opposite of the T-chevrons, although not quite mirror-symmetric about the horizontal axis due to the presence of the pylon on the top side.

Further, although our argument for enhanced mixing between fan and ambient flows suggests examining these AVCs mainly for the fan nozzle, we also need to examine these AVC concepts on core nozzles which would affect the mixing not only between the core and the fan stream, but also further downstream where it affects the mixing with the ambient flow. Thus, we can have T-fan, T-core, B-fan and B-core chevrons too. Together with the regular R-chevrons, we can mix and match all these three types of chevrons (R, T and B) on both fan and core nozzles or keep one of them as baseline simple splitter nozzle, if desired, for a systematic study. Figure 3 shows some examples of these AVC combinations.

III.   Nozzle Models, Experimental Facility and Acoustic Instrumentation

A. Isolated Nozzle Models
The baseline simple splitter (no chevron) nozzle was chosen to be typical of a modern high bypass ratio engine (with take-off bypass ratio of around 7) and scaled down so that it can be installed on the internal jet rig in Boeing's Low Speed Aeroacoustic Facility (LSAF), which is described later. The nominal value of the fan to core area ratio is 3.34. The state-of-the art azimuthally uniform reference R-chevrons were designed using best design practices for both fan and core nozzles, and had 16 and 8 chevrons, respectively. In practice, we cannot use the full circumference of the nozzle for the fan chevrons due to the pylon on the top side and also the thrust reverser sleeves on the bottom side of the fan nozzle – resulting in a loss of "azimuthal real-estate" from the point of view of enhancing mixing with chevrons. Similarly, for the core nozzle the presence of the so-called "heat-shield" at the bottom of the pylon (used to prevent the pylon sides from getting scorched by the hot core flow) prevents utilizing that azimuthal region near the pylon for core chevrons. This loss of azimuthal space can be as high as 90º to 100º totally around the circumference for each nozzle, and needs to be accounted for when designing such chevrons on scaled nozzles. Such pylon related installation issues were not a concern in the original studies of chevrons.

The T- and the B-azimuthally varying chevron nozzles, for both fan and core nozzles, were designed with approximately these R-chevrons as reference chevrons in roughly the middle portion (between top and bottom) of the nozzle and different chevrons on top and bottom. For the sake of comparison with the R-chevrons, both T- and B-fan nozzles had 16 chevrons, and T- and B-core nozzles had 8 chevrons; the chevron chord lengths (from root to tip) and the immersion angles (measured between the tangent at root and the chord) varied approximately linearly from top to bottom. Due to lack of time, only a very rudimentary one-dimensional flow analysis was done, rather than a comprehensive three-dimensional CFD simulation, to make the effective areas of these AVC nozzles same as their baseline counterparts at cruise conditions. In particular, note that the AVC nozzles that were finally fabricated and tested are only specific instances of AVC nozzles for studying the proof-of-concept and no attempt was made to optimize their shape or size from the viewpoint of aerodynamic performance.

For the isolated nozzle test phase of this program we used two fan AVC nozzles (T and B) and two core AVC nozzles (T and B) besides the conventional reference (R) fan and core chevron nozzles, and simple round baseline (b) nozzles. The different chevrons on fan and core nozzles were made as nozzle rings which could be interchanged, thus providing a wide variety of nozzle combinations. The complimentary installed nozzle test in Part 2 on the other hand, had few more variations of AVC nozzles and a group photo of all these nozzles can also be found in Part 3.

B. Experimental Facility
All these nozzle combinations were tested in the NTL3800 jet noise simulator in Boeing's Low Speed Aeroacoustic Facility (LSAF). LSAF is an open jet wind tunnel in a premier quality large anechoic chamber measuring 65 ft by 75 ft by 30 ft. The chamber is lined with foam wedges that allow free field measurements to be made between 200 Hz to 89,000 Hz. For this test, a 7 ft by 10 ft contraction exit insert was installed on the wind tunnel to allow it to achieve a maximum Mach number of 0.32. The free jet exhaust is through 19 ft by 19 ft exhaust collector. The NTL3800 is a dual-flow nozzle simulator used for jet noise testing. It is designed to operate at a

maximum temperature of 1500ºF for the primary stream and at a maximum temperature of 250º F for the secondary stream at a flow rate of 30 lb/sec dual flow. Model boundary layer control is accomplished by pulling a vacuum across fine wire mesh cone that installs upstream of the model and replaces the rig outer wall. Further general description and figures of LSAF and the hot jet simulator rig can be found on Boeing's website[††].

(a) Nozzle in free-jet wind-tunnel   **(b) Close-up aft view**

Figure 4. Isolated RT-nozzle with a pylon (near 9 o'clock position) installed in Boeing's LSAF jet rig.

Figure 4 shows two views of the isolated nozzle model RT (that is, R-core chevron nozzle and T-fan chevron nozzle) with the pylon mounted on this jet simulator in LSAF. The pylon is slightly tilted to the horizontal plane by an angle of 6º to accommodate an almost vertical wing attached to it with a slight tilt (due to its dihedral angle) in the companion installed-nozzle testing phase of this program.

C. Acoustic Instrumentation & Phased Array Data Processing

There were three arrays of far field microphones at different azimuthal angles used in this test program but only the one which is used in this paper is described further. Thirteen microphones were tower mounted in a polar array pattern in a horizontal plane at an azimuthal angle, which will be referred to as 0 degrees[‡‡]. These microphones were distributed at polar directivity angles ranging from 60 to 150 degrees, as measured from the jet inlet axis, on a polar arc of radius 25 feet from the baseline primary nozzle exit plane center. There was a microphone at every 10º in the 60º to 120º range, and then every 5º from 120º to 150º. The polar microphones are 32.1 fan diameters or 68.7 core diameters from the core nozzle exit center, and although not *ideally* at a far field distance it is considered to be at a *reasonably* far field distance. Data requirements for this test included steady-state one-third octave band and narrowband data from 200 Hz to 89 kHz.

For source diagnostics purposes, we used phased microphone arrays outside the wind-tunnel flow. The phased array consisted of 117 Brüel & Kjær ¼-inch type 4938-W-001 microphones flush mounted in a vertical flat plate positioned b = 97.4 inches horizontally from the core nozzle exit plane center (b/D$_{core}$= 22.30). The verticle plate, which was attached to a cart, was mounted on a horizontally traversing track (parallel to the wind tunnel flow direction) and allowed for a range of phased array positions relative to the nozzle exit plane. Phased array measurements were generally acquired with the line-of-sight from the array centroid to the core exit plane at 90º directivity angle. Supplemental measurements were obtained with this line-of-sight at 125º, and a small number of measurements were obtained at 52º and 70º. When acquiring far-field acoustic data, the cart was traversed to a stow location behind the tunnel contraction.

Figure 5 shows the spatial distribution of the phased microphone arrays. As indicated, the microphones were configured into two subgroups: the "large array" microphones (red circles) were used for sampling the larger spatial

---

[††] http://www.boeing.com/commercial/techsvcs/boeingtech/bts_acoub.html
[‡‡] This horizontal microphone array position is referred to as 0 degrees azimuth because the microphones can be considered directly "under" the engine pylon, although the pylon in our jet-rig setup is actually rotated 84º counter-clockwise from the top dead center as shown in Fig. 4.

wavelengths (frequencies of approximately 1 kHz to 12 kHz), and the "small array" was used for the shorter spatial wavelengths (roughly 10 kHz to 20 kHz). Note the sharing of microphones between subgroups. The large and small arrays contained 81 microphones each. The microphones for a given array were distributed along nine logarithmic spirals according to design principles given in Underbrink[16].

The microphone data from the phased array was sampled at 196,608 samples per second for a period of 10 seconds. Cross-spectral matrices were created from the time series data in $1/12^{th}$ octave bands and beamformed using conventional beamforming methods[17]. Refraction of sound by the wind-tunnel shear-layer was accounted for in the processing. It is known that when such beam-forming method is used for planar arrays, the spatial distribution of the source "in front" of the array (that is, on the normal to the array plane through its centroid) is well captured; sources to either side of this normal appear slightly skewed with the distortion increasing when the line-of-sight from the centroid goes further and further away from the normal; yet the peak source location and amplitude are well captured.

Figure 5. Spiral arrangement of microphones on a vertical plane for two sets of phased arrays for source diagnostics.

Since the 90º-phased array is placed at a sideline distance of 97.4 in. from the nozzle axis, the angle away from this normal is given by $\tan^{-1}(0.0448L/D_{core})$ where L is the axial location of the source from the core exit plane. For example, for $L/D_{core} = 10$ this gives an angle of 24º away from the normal and some distortion is expected, but for a source at the nozzle exit plane, L = 0, no distortion is expected. Moreover, our comparison of data with a synthetic source location at $L/D_{core} = 10$, which has less deviation from the normal for the 125º array location than the 90º array location, shows that this spatial distortion for the 90º array is minimal and the source location diagnosed is hardly changed; on the other hand, for the 125º-array location the source at the nozzle exit plane is grossly distorted. Hence, the 90º array location best captures both the source locations from amongst the four phased-array locations used, and is more suitable for capturing both low and high frequency sources. Only data taken from the 90º array-centroid location is presented here for brevity.

Further, it should be noted that sources located by the 90º-array will correspond to a line-of-sight in the far field which passes through the source and the array centroid; thus, sources at the core exit plane correspond also to approximately 90º directivity angle in the far field polar array, but sources downstream of the core exit plane correspond to the upstream quadrant in the far field. When there is no tunnel flow (static conditions) the line-of-sight and the ray from the source to the centroid, of course, coincide. Thus, for example, for a source at $L/D_{core} = 10$ the line-of-sight angle with the nozzle axis is 65.9º which corresponds to a far field (R = 25 ft) microphone directivity angle of 73.5º. After accounting for refraction due to wind-tunnel shear layer, if the wind-tunnel flow is on, hence, such a downstream source found by the 90º-array will correspond to a polar angle which is even less than 73.5º. This should be kept in mind when comparing results from this phased array to the far field polar array.

The beamforming grid is 104 inch by 35 inch in extent and contains, respectively, 429 by 1445 grid points for the small spiral array, and 573 by 193 points for the large spiral array processing. The worst case side-lobe levels for the array pattern are about 10 dB below the main lobe peak for both the large and small arrays up to 59 kHz and 9.5 dB up to 88 kHz. For beam map image clarity, the SPL contour-plot image dynamic range was restricted to 8 dB below the peak level in a given beam map. This was done to reduce the possibility of mistaking array side-lobes for actual sources. The repeatability of peak SPL values from the large spiral array is consistently high and is within ±0.15 dB for frequencies between 1223 hz and 12232 hz, and the data only from this array is reported here.

IV. Experimental Results

Table 1 shows the various chevron and baseline nozzle combinations that were tested in the isolated nozzle configuration. It should be noted that the isolated test reported here was chronologically done after the installed test of Part 2 for certain logistic reasons, like availability of the installed nozzle setup at the beginning of the test

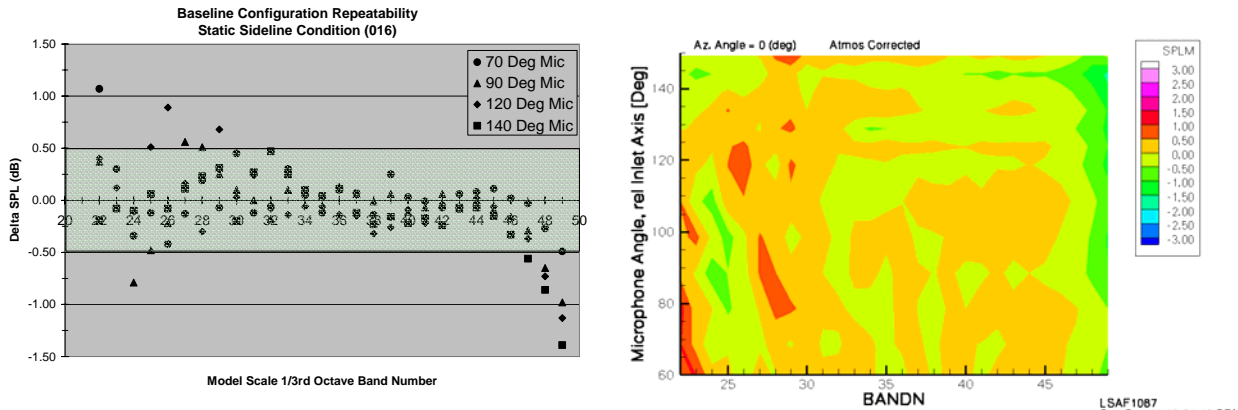**Table 1. Isolated nozzle test matrix of combinations of fan and core chevron nozzles.**

FAN CORE	b	R	T	B
b	bb		bT	
R		RR	RT	
T			TT	
B	Bb	BR	BT	BB

program, etc. Thus, we could selectively test the isolated nozzle combinations, and the test matrix in Table 1 does not appear fully populated. It is possible to extract the acoustic effect of, say, the fan AVC nozzles by keeping the core nozzle the same, such as, b, R or B; or, to study the effect of the core AVC nozzles by keeping the fan nozzle the same, such as, b, R or T. Some of these effects due to AVC variation are analyzed here.

Most of these nozzles were tested for several engine cycle conditions typical of modern high bypass turbofan engines covering mainly take-off conditions at full and cutback power at wind-tunnel Mach numbers of $M_{wt} = 0.0$ and 0.30, and also low-power approach conditions at $M_{wt} = 0.0$ and 0.24 for studying the effect on community noise. However, in this paper results for only one take-off power condition are reported, which is nominally, $NPR_f = 1.735$, $NPR_c = 1.622$ and $TTR = 2.513$ with $M_{wt} = 0.30$. At this take-off condition, the nominal bypass ratio is 6.9, the nominal ratio of fan to core speed is 0.67 and that of ambient to fan speed is 0.32. Before presenting the AVC effects we first show data repeatability and wind-tunnel noise floor so that we know the frequency-angle range of data usability.
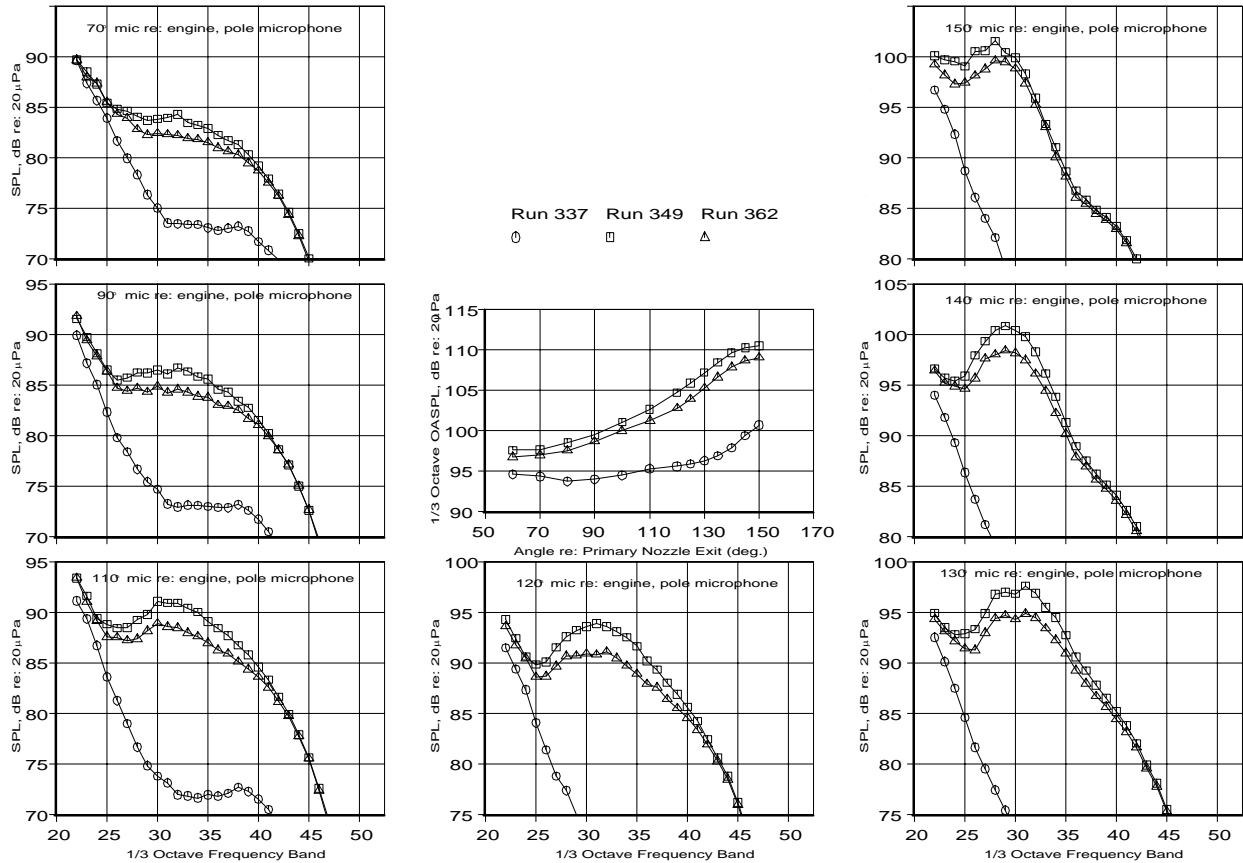
A. Data Repeatability and Wind-Tunnel Noise

(a) Data scatter in SPL spectra between two repeat runs at several angles

(b) Data scatter in SPL between repeat runs for the observable spectral-directivity plane
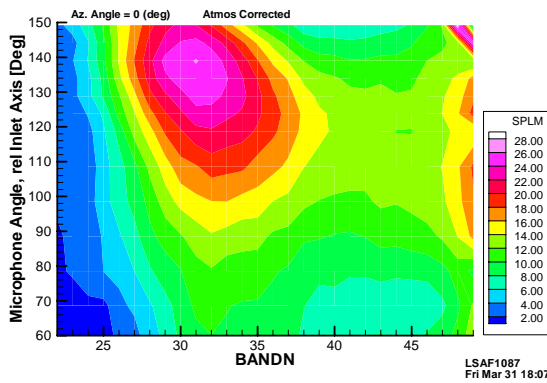
Figure 6. Far field SPL data repeatability for the isolated baseline nozzle, bb, at static sideline power conditions (016) as a function of 1/3rd octave band number (17 to 49) and microphone angle (60º to 150 º).

Test conditions for the baseline (bb) configuration and some AVC nozzles were repeated often to examine the variability in the test data throughout the test period and, thus, obtain a limit on data scatter at different frequencies and angles. All the far field test data was normalized to the standard acoustic day conditions (T = 77º F, RH = 70%, $p_{amb} = 14.7$ psi) using the well-known Bass-Shield atmospheric corrections[§§] so that comparisons could be made between any two configurations. Figure 6 shows an example of such SPL data scatter for the bb-nozzle under static conditions ($M_{wt} = 0.0$) for two repeat tests a week apart: Fig. 6(a) shows that the SPL scatter for mid-to-high
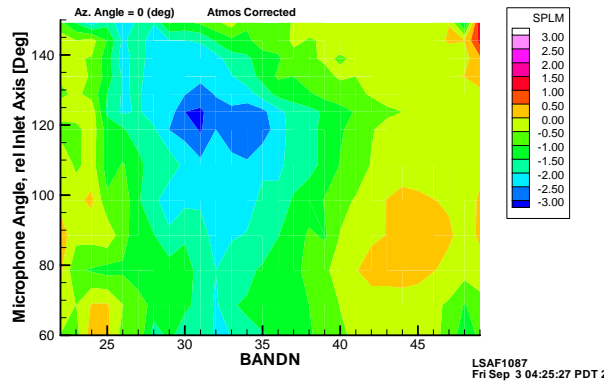

[§§] In this paper, we use the "simple" standard atmospheric correction which assumes that the jet noise source is at the core nozzle exit center and the correction distance is simply the distance from the core exit plane center to the microphone (R = 25 ft); this causes only minor differences from the more elaborate atmospheric correction scheme which assumes the same core exit plane as the source location but uses appropriate refracted path through the wind-tunnel shear layer and the corresponding flow properties. For static wind-tunnel conditions there is no difference between these two corrections.

(a) SPL and OASPL comparison of bT, bb and wind-tunnel noise

(b) Difference in SPL between baseline nozzle, bb, and wind-tunnel noise

(c) Difference in SPL between bT and baseline nozzle, bb

Figure 7.   Effect of T-fan nozzle with baseline core nozzle, bT, (run 362) in comparison to the baseline nozzle, bb, (run 349) and wind-tunnel noise (run 337) at $M_{wt} = 0.3$.

frequencies (band 27 to 47) is within ±0.5 dB for all microphone angles shown, but it falls off beyond this range for very low frequencies (band < 27) and very high frequencies (band > 47); Fig. 6(b) shows the difference in SPL

between the two repeat runs across the whole spectral-directivity plane as a contour plot, and confirms that the ±0.5 dB limit (golden and light green color) is applicable, in general, to the above range of band numbers and microphone angles although there may still be a few outliers. (This comprehensive method of plotting is the preferred way of presenting SPL difference data in this paper[***].) Note, from Fig. 6(a), that for mid-frequency range of band numbers between 33 and 45 this scatter is even much tighter, approximately 0.3 dB or so. This was seen in almost all the repeat tests with other configurations. So we consider ±0.5 dB as the repeatability band for SPL data within $1/3^{rd}$ octave-band numbers 27 and 47 for all angles for this test.

Figures 7(a) and 7(b) show a comparison of SPL for the baseline bb-nozzle at take-off power conditions with M_{wt} = 0.30 and when just the wind-tunnel is on at M_{wt} = 0.30 (without the model jet being on). These figures show that the wind-tunnel noise floor is considerably lower than the model jet noise at these high power conditions everywhere, except for the very low band numbers in the upstream quadrant. This observation combined with the frequency range imposed by SPL data scatter band of ±0.5 dB, mentioned earlier, gives a reasonable confidence in the LSAF data repeatability over most of the angular and frequency ranges of interest, with the exceptions noted.
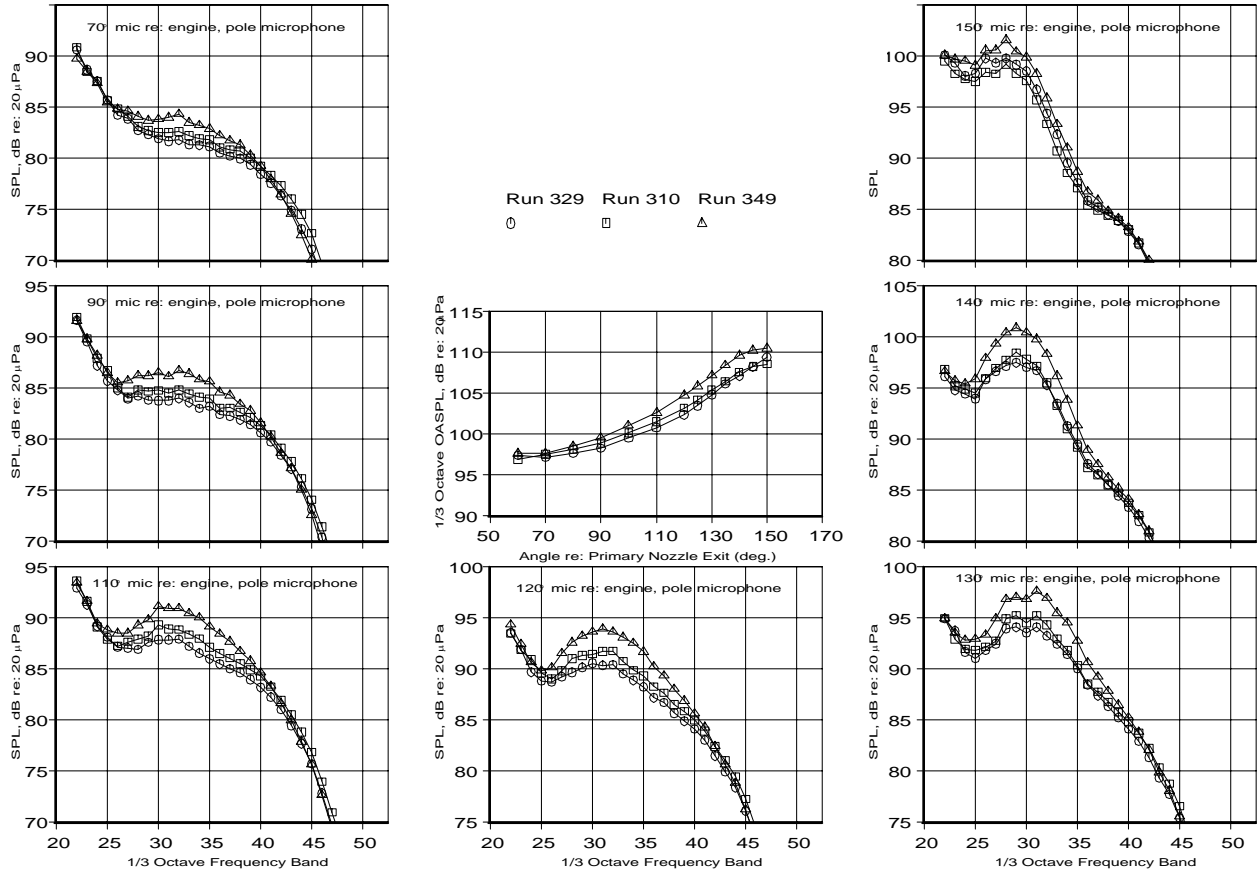
B. Isolated Fan AVC Effect

Figures 7(a) and 7(c) show the effect of the T-fan chevron nozzle alone, bT, that is, with a baseline core nozzle, in comparison to the baseline nozzle (bb) in terms of SPL line and contour plots, respectively. These figures show more than 2 dB reduction for low frequencies (band 27 to 36, or frequencies from 500 hz to 4000 hz) in most of the aft quadrant. The maximum reduction of 2.5 to 3 dB is found between 110º and 130º although the peak SPL still occurs at the very shallow angles around 150º. This is particularly notable because no high-frequency lift (HFL) in SPL, which is so endemic to conventional chevrons, is seen in the T-fan chevrons.

It is of immediate interest to see then what happens when we add a conventional R-core chevron nozzle to the T-fan nozzle, that is, RT-nozzle, and compare it with the conventional RR-nozzle. Figure 8 shows this comparison between RR and RT nozzles and the SPL difference with respect to bb-nozzle. We note the following points:
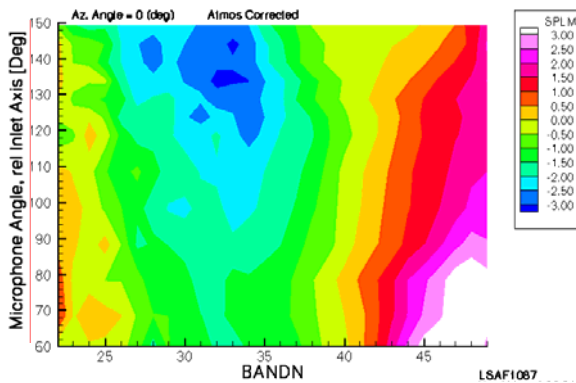
a) Fig. 8(b) shows that the RR-nozzle reduces the SPL in the aft quadrant from 2.5 to 3 dB and increasingly so for wider and wider frequency band range as we go aft; however, it comes at the price of HFL beyond band 41 (12.5 kHz) or so, especially in the front quadrant.

b) Note from Fig. 8(a) that at these high frequencies (band > 41) the SPL is far below the peak SPL value at any given angle, but for practical full-scale applications where the noy penalty for perceived noise levels is larger at high frequencies (near 3 kHz full-scale) HFL can be detrimental. However, in real engines there are noise sources at these high frequencies and forward angles other than jet noise, such as, fan noise, etc. which can dominate. HFL from jet noise still will increase the broadband noise floor and is generally considered detrimental.

c) Fig. 8(c) shows the relatively large SPL reduction (big dark-blue "island" in the spectral-directivity plane) obtained by the RT-nozzle in comparison to the baseline nozzle. It is beyond 3 dB over most of the aft quadrant for bands 30 through 36, and from Fig. 8(a) is seen to gain a maximum of about 3.8 dB reduction around 120º microphone angle. There is some HFL in the upstream quadrant but the bands where it occurs is pushed to a much higher limit (band > 44) compared to RR.

d) Comparing Figs. 8(b) and 8(c), we see that the RT-nozzle is much quieter than the conventional RR-nozzle, and the difference can only be due to the T-fan azimuthally varying chevrons, since the R-core chevrons are the same in both cases. On the other hand, comparison between Fig. 8(c) and 7(c) shows that the culprit for the HFL in RT-nozzle must be the R-core nozzle, not the T-fan nozzle, although with the same token the R-core nozzle also helps to reduce the low frequency noise further.

e) Fig. 8(c) is, perhaps, the most important and useful finding in this paper.

Now let's compare the effect of all types of fan AVCs keeping the core chevron nozzle the same. From Table 1 we see that it can be done for the last row with B-core chevrons the same and varying the fan nozzle as b, R, T, and B. Figures 9(a) through 9(d) show this comparison for Bb, BR, BT and BB nozzles, respectively, in terms of SPL difference with respect to the baseline nozzle, bb, at the same take-off conditions. We note the following points:
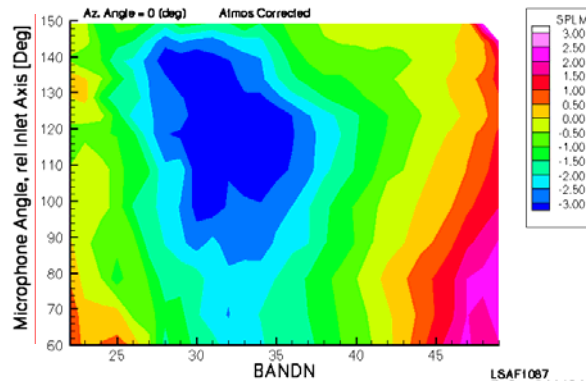

[***] Note that when the wind-tunnel Mach number is the same for any two comparison configurations which have their nominal core exit plane at the same axial location, each microphone angle corresponds to the same emission angle in the two configurations assuming the source is at the core exit plane center. Hence, although it is usually preferable to use emission angle for comparison across different test facilities or different tunnel Mach numbers, in general, using microphone angle for comparative purposes in the same facility at same tunnel Mach number, as done here, is not inappropriate.

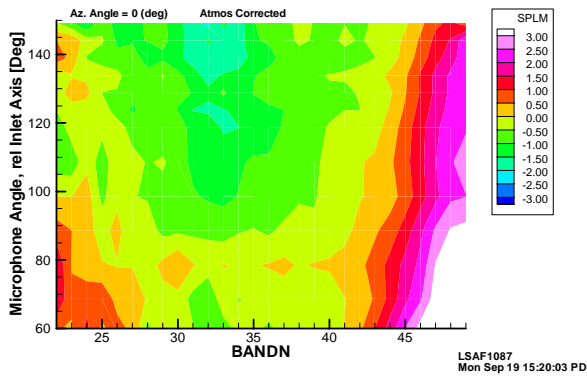(a) SPL spectral comparison at various directivity angles and OASPL directivity

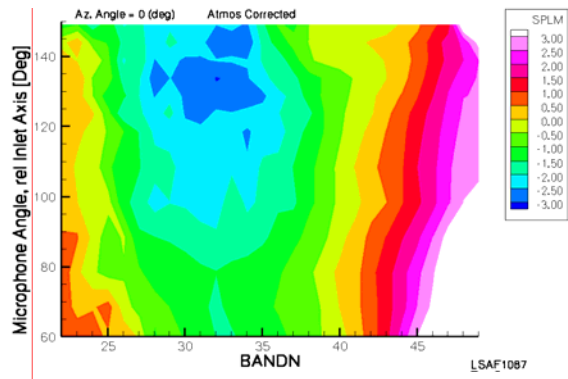(b) Difference in SPL between RR and baseline nozzle, bb

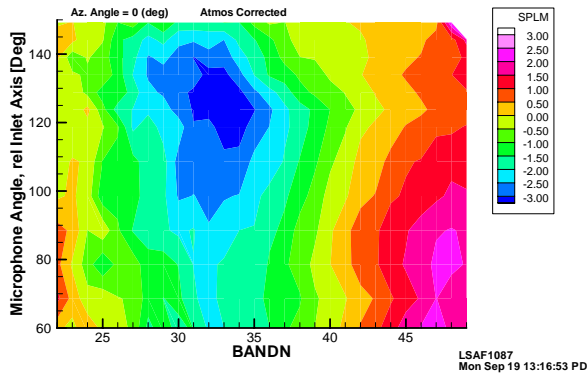(c) Difference in SPL between RT and baseline nozzle, bb

Figure 8. Comparison of RT (run 329), RR (run 310), and bb (run 349) nozzles at $M_{wt} = 0.30$.

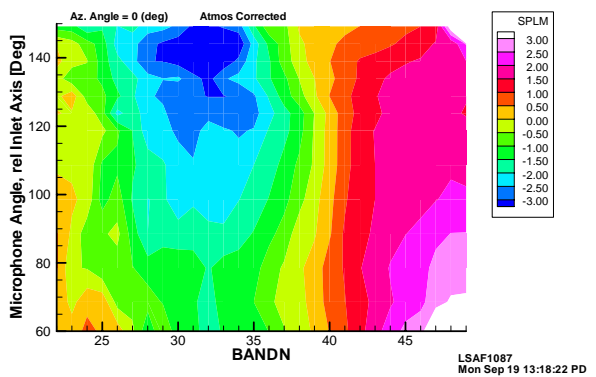American Institute of Aeronautics and Astronautics
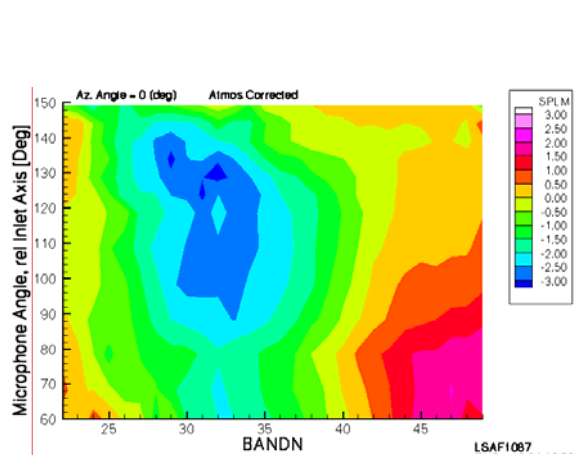
(a) Bb (run 451)

(b) BR (run 447)

(c) BT (run 434)

(d) BB (run 443)

(e) TT (run 373)

Figure 9. Difference in SPL between several combinations of azimuthally varying core and fan chevron nozzles and the baseline nozzle (run 349) at M_{wt} = 0.30.

a) Fig. 9(a) first shows that the B-core chevron nozzle alone (with baseline b-fan nozzle) reduces the SPL somewhat in the aft region (about 1 to 1.5 dB) but not as much as the previous T-fan chevrons alone (Fig. 7(c)); moreover, the B-core chevrons come with a fairly high HFL.

b) Figs. 9(b) and 9(c) show that the noise progressively reduces as we add R-fan chevrons and then T-fan chevrons. Comparison between them shows that the T-fan chevrons, when used in conjunction with the B-core chevrons, not only reduce the low frequencies but also have a "calming" effect on the HFL. It is also evident from comparing BR vs. BT or RR vs. RT (compare Figs. 8(b) and 8(c)) that whenever T-fan chevrons are used, the peak SPL reduction appears at slightly lower angles than it is for the conventional R-fan chevrons. The BT-nozzle is also quieter than the conventional RR-nozzle (compare Fig. 9(c) and 8(b)), but perhaps not, perhaps, as quiet as the RT-nozzle.

c) Lastly, Fig. 9(d) shows that when both fan and core nozzles have B-chevrons (BB-nozzle) the HFL is across all angles and begins earlier in terms of frequencies, at band 40; however, the low frequency reduction is still slightly better than the conventional RR-nozzle (compare dark-blue footprint areas in Figs. 9(d) and 8(b)).

C. Isolated Core AVC Effect

From Table 1, we see that this effect of changing the core chevrons can be studied, keeping fan nozzle the same, from nozzle combinations in three columns, namely, (i) bb vs. Bb (already discussed above), (ii) RR vs. BR, and (iii) bT vs. RT vs. TT vs. BT. Most of the SPL difference results in comparison to the baseline nozzle have already been shown earlier for these nozzle combinations, except for TT which is shown in Fig. 9(e). From Fig. 9, we note:

a) Comparison of Figs. 9(b) and 8(b) for BR vs. RR nozzles shows that keeping conventional R-fan chevrons the same, and changing the core chevrons from R to B, does not change the low frequency reduction much, but increases the HFL instead. Hence, B-core chevrons are not to be preferred over R-core chevrons.

b) Comparison of Figs. 7(c), 8(c), 9(e) and 9(c) brings out the effect of core chevrons keeping T-fan chevrons the same. The important generalized statement that can be made first is that all these nozzle combinations, with the T-fan chevrons as the common element, appear quieter than the conventional RR-chevron nozzle (Fig. 8(b)) in terms of low frequency reduction and HFL, with RT-nozzle as the quietest. bT and RT-nozzles have already been compared earlier. As the core nozzle changes from B-chevrons to T-chevrons, (BT vs. TT), it appears that the HFL decreases but the low frequency reduction remains almost the same.

D. Source Diagnostics

The changes in far field noise that we have studied in the above two sections must be related to the changes in the structure of the jet plume due to the different azimuthal mixing patterns imposed by fan and core AVCs, and its interaction with the flow behind the pylon. In single-stream nozzles with conventional azimuthally uniform chevrons but no pylon, it is known that enhanced mixing, which leads to larger spreading angles of the shear layer, consequently reduces the potential core length. One can extend this argument to AVCs in single-stream nozzles, and hypothesize that in sectors where the mixing is enhanced by the larger or more immersed chevrons, the spreading angle of the shear-layer must be high and the potential core length in the corresponding sector should be smaller, whereas, the opposite must be true where there is less mixing. With top-to-bottom asymmetry imposed on these AVC this implies that the potential core must be skewed.

This simple reasoning, however, may not be applicable in a straightforward manner for coaxial nozzles and, especially, when a pylon that bifurcates the fan flow is present. This will have to await either experimental flow measurements or an appropriate CFD analysis. A full CFD analysis of the RT-nozzle with the pylon was completed recently, after this test was over, and is reported in Massey et al[18], and throws some light into the complex flow/noise characteristics of such AVC nozzles. During the test program in 2004, however, we resorted to a phased array of microphones as our acoustics source diagnostics tool.

In general, it is known that the jet noise source at most low frequencies is spread in the axial direction, although there may be some localization after the potential core ends. It is interesting to compare the locations of the dominant sources and their amplitudes for the AVC nozzles at different frequencies with those for the baseline and conventional chevron nozzles and see if they corroborate the far field data.

Figure 10 shows a comparison of source diagnostics for the baseline nozzle, bb, and the bT-nozzle (with T-fan chevrons alone) at several frequencies as measured by the 90°-phased-array. Before we start analyzing these plots, a few notes on the color-contouring scale used in these phased-array plots:

1.   The SPL values shown are as received by the 90°-array at the array location, not at the source location.

2.   For a given frequency we use the same color scheme for both configurations, that is, the same color in both configurations implies the same absolute SPL value in both plots – the maximum value of the color scheme
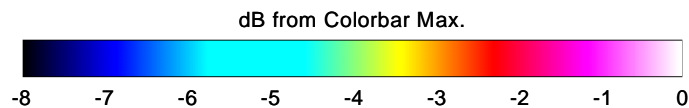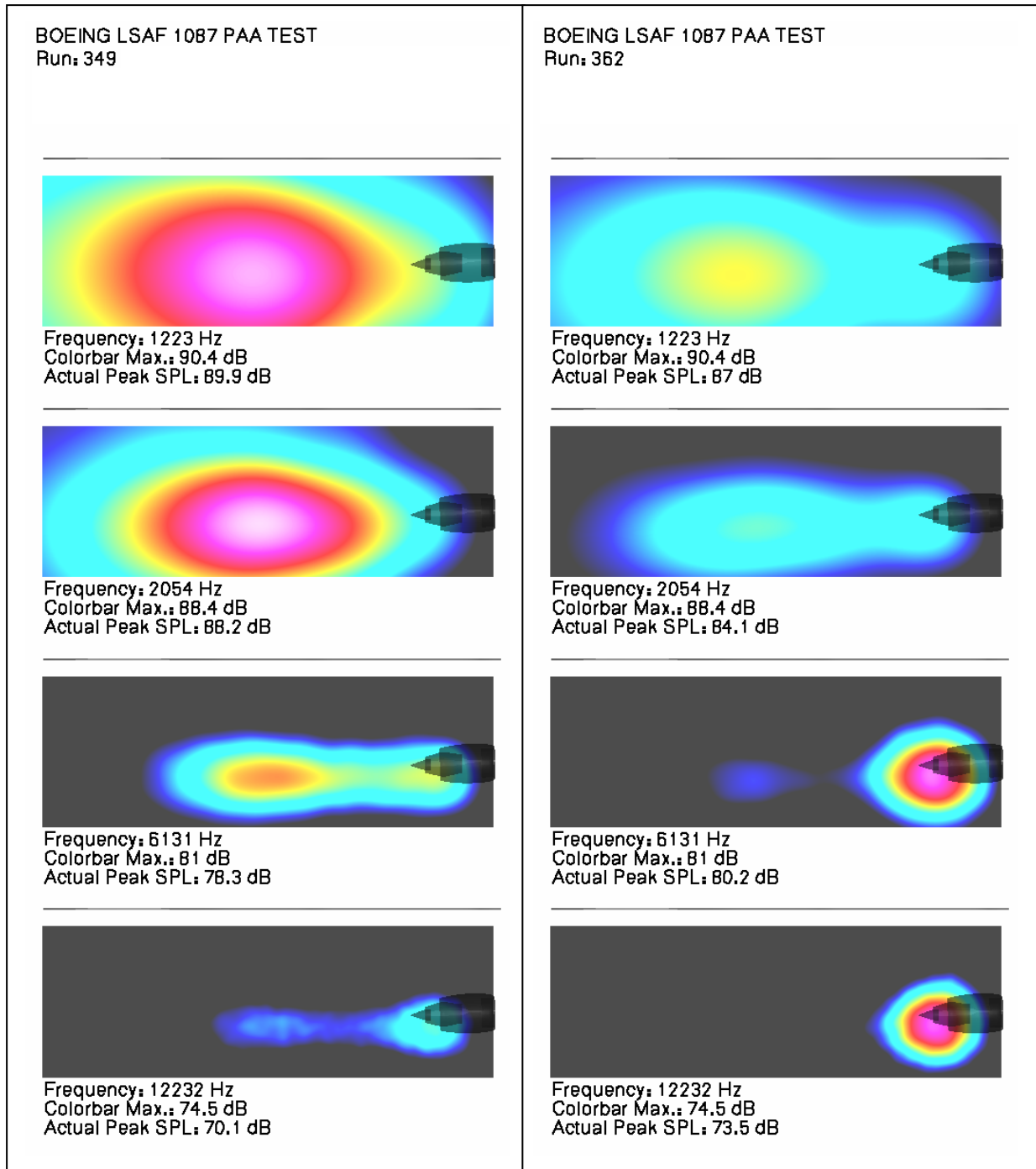
Figure 10. Source diagnostics comparison between (a) baseline nozzle, bb (Run # 349), and (b) bT-nozzle (Run # 362) as "seen" by the phased array with centroid at 90º for several frequencies.

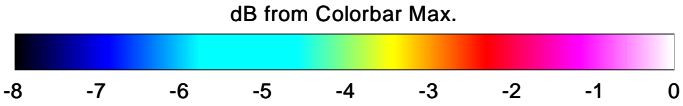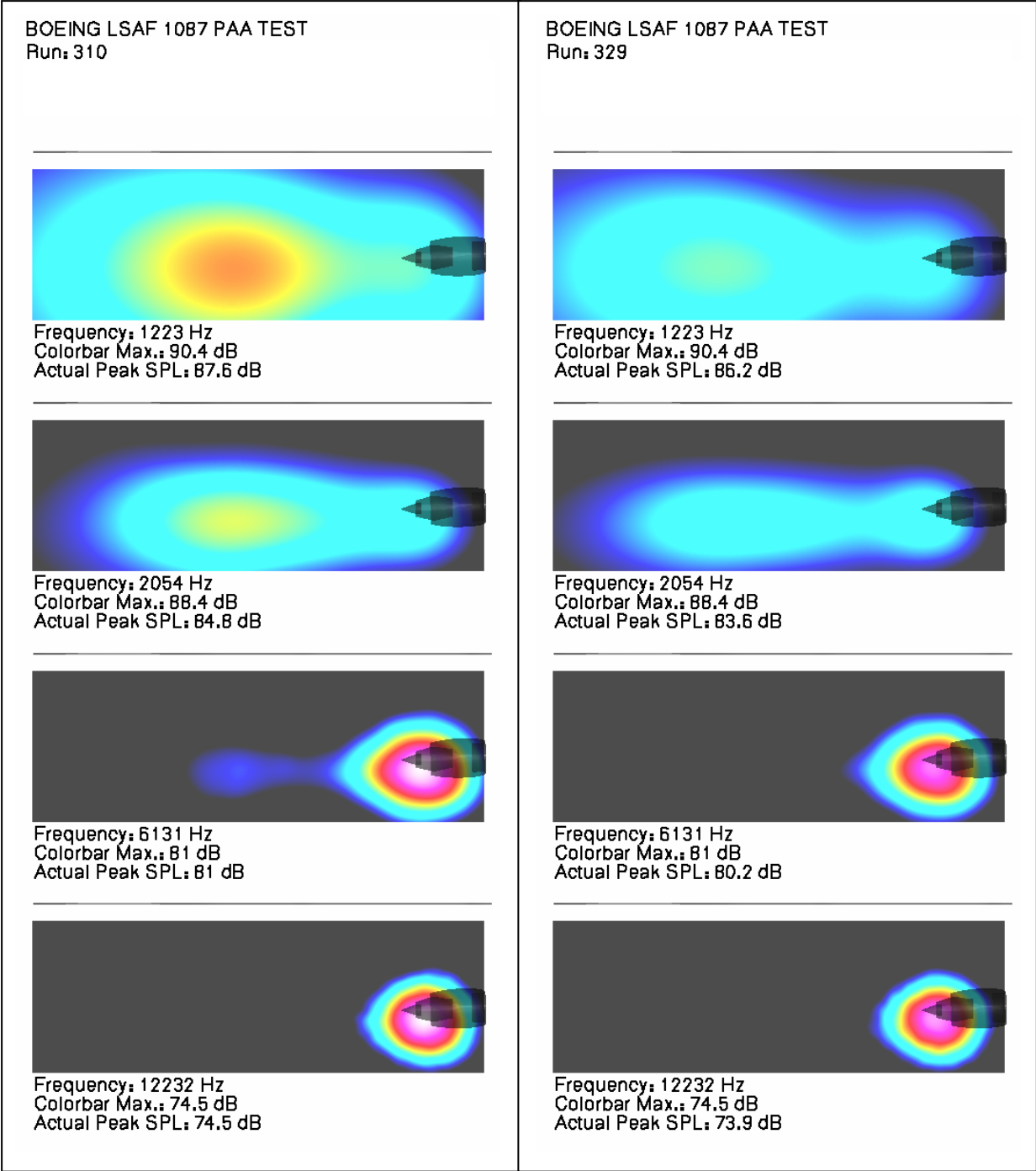American Institute of Aeronautics and Astronautics

Figure 11. Source diagnostics comparison between (a) RR nozzle, bb (Run # 310), and (b) RT-nozzle (Run # 329) as "seen" by the phased array with centroid at 90º for several frequencies.

(white) being designated as "Colorbar Max" under each plot; the actual peak SPL value occurring in each plot is also shown under each plot and can be different than the Colorbar Max value.

3. The "Colorbar Max" value for each frequency can be different

4. The remaining absolute SPL values in a given plot are to be found from a difference SPL color scale shown at the bottom and is common for all plots. Thus, the actual SPL value at a given location (for a given plot) = Colorbar Max (for that plot) + ΔSPL for that location (using common color scheme at the bottom).

Thus, the first row in Fig. 10, at 1223 hz (band = 30.9), for the bT-nozzle shows a downstream peak source reduction of 2.9 dB, with considerable reduction over a widespread region in the jet plume. This, indeed, agrees with the far field reduction of more than 2 dB near 70º-75º directivity angles for bT-nozzle which receives sound from the whole jet plume (see Fig. 7(a) or 7(c) and previous discussion of why 90º-array centroid position corresponds to 70º or so of far field angle on the far field polar array). At 2054 hz (band = 33.1), a significantly larger SPL peak reduction of 4.1 dB is seen (second row, Fig. 10). It is, indeed, for these band levels (30 to 35) that the largest far field SPL reduction was observed earlier in Fig. 7(c) at all angles, especially, around 120º; however, to corroborate that we would need the phased array source data at the corresponding centroid position, but is not available. However, even in upstream quadrant, near 70º-75º this reduction in far field is still evident (see Figs. 7(a) and 7(c)). At still higher frequencies of 6131 hz (band = 37.9) and 12232 hz (band = 40.9), Fig. 10 shows that the dominant source for bT-nozzle shifts to the nozzle exit plane; whereas, for the baseline nozzle it is still seen to be in the downstream plume for, at least, 6131 hz. Also, the exit-plane source for bT-nozzle now has a higher peak SPL value than the dominant source for the baseline nozzle which, however, remains downstream.

These source diagnostics plots amply capture the two dominant sources, one for low frequencies which is downstream and the other for high frequencies which is dominant near the nozzle exit plane. These have a great resemblance to the low frequency sources associated with the well-known large-scale instabilities, which are dominant downstream of the potential core, and the high frequency sources associated with the fine-scale turbulence near the nozzle exit plane. Since the source grid plane, shown in Fig. 10(b), includes the chevrons between the pylon and the bottom of the nozzle (recall the pylon is "away" from the phased array or on the "other" side of this grid plane), Fig. 10(b) directly captures how these mid-chevrons produce higher source intensities at higher frequencies near the nozzle exit plane but which are not evident in the far field (see Fig. 7(c) near 70º-75º), possibly due to atmospheric attenuation. These plots, shown at progressively increasing frequencies, also imply that there must be an intermediate frequency, different for each nozzle, where both downstream and upstream sources have the same magnitude.

Now let us compare the conventional RR-chevron nozzle and the RT-nozzle which proved to be the quietest in the far field amongst all the AVC nozzles studied. Figure 11 shows the phased array plots for both of them and, for comparative convenience, we have used the same color scheme and Colorbar Max values for each frequency as for bb and bT nozzles shown in Fig. 10. For the lowest frequencies shown (1223 hz and 2054 hz) it is immediately clear that the RT-nozzle has the lowest noise source levels amongst these four nozzles; the RR-nozzle has higher noise source than even the bT-nozzle. At the higher frequencies of 6131 hz and 12232 hz, the dominant source for RR and RT has moved to the nozzle exit plane, just like the bT-nozzle, but the RT-nozzle sources are still less in magnitude than the RR-noise sources. In comparison to the bT-nozzle sources, the RT-nozzle source is equal in magnitude at 6131 Hz but slightly higher at the highest frequency (12232 hz) which implies that it may be due to the R-core chevrons. RT-nozzle also has higher source noise than bb nozzle at the highest frequency but it is not seen in the far field (see Fig. 8(c)), again possibly due to atmospheric attenuation.

Table 2 summarizes the peak SPL magnitudes, as well as the axial locations of the "downstream" source (which is not always the dominant source at each frequency) from these phased-array plots for all the four nozzles: bb, RR, bT and RT. As we have already noted earlier, there is a monotonic decrease in this source level as the T-fan chevrons are introduced, first on their own (bT, without the R-core chevrons) and then in conjunction with the R-core chevrons (RT). For the two lowest frequencies shown, where the downstream sources dominate for all nozzles, the decrease in peak SPL due to RT-nozzle can be as high as 4.7 dB. More interesting is the movement of the axial location of the peak low-frequency sources with the introduction of the T-fan chevrons: at 1223 hz, it moves further *downstream*, compared to bb-nozzle, from x/D_{core} of 9.0 for bb to 10.3 for bT and 11.3 for RT and, similarly, at 2054 hz it moves from 8.6 for bb to 9.1 for bT and 10.5 for RT.

From the earlier discussion, since the T-fan chevron nozzle enhances mixing on the top side (near the pylon) more than the baseline nozzle, one would expect the secondary potential core length to decrease there, but the one near the bottom should be longer than the top portion due to decreased mixing. It is expected that this would skew the secondary potential core; but its effect on the primary potential core is difficult to extrapolate particularly due to the presence of the pylon, which with its bottom shelf can deflect the core stream upwards and result in a fairly complex flow downstream, as seen in earlier CFD studies[7, 9]. The source data for RT-nozzle (see Table 2), on the other hand, shows that the peak low-frequency source, as seen by the 90º-phased array, has moved further downstream than it is in the baseline nozzle case, and in the process has become weaker than similar sources in the baseline or even the conventional chevron nozzle. The flow-physical reason as to why such skewing of the

**Table 2. Peak SPL strength & source location of the downstream source as seen by
90º-phased array during isolated nozzle test at sideline power.**

Isolated Nozzles @ SL-Power		Downstream Source Peak SPL @ 90º Array (dB)				Downstream Source Location $(x/D)_{primary}$			
freq. (hz)	10log(freq)	bb	RR	bT	RT	bb	RR	bT	RT
1223	30.9	89.9	87.6	87.0	86.2	9.0	9.4	10.3	11.3
2054	33.1	88.2	84.8	84.1	83.5	8.6	9.4	9.1	10.5
6131	37.9	78.3	74.2	74.2	72.8	7.7	9.2	9.3	10.0
12232	40.9	70.1	64.4	64.0	63.0	7.4	8.8	7.4	9.7

secondary potential core, in the presence of the pylon, would cause axial shift downstream or delay and weakening of the most dominant noise source in the coaxial jet plume needs to be explored further. It would also be interesting to see if this happens with the T-fan chevron nozzle alone in the absence of a pylon. Some insight into the fundamental flow and noise mechanisms can be obtained from detailed computational flow and noise simulations done recently for the RT-, RR- and bb-nozzles by Massey et al.

V.   Conclusion

We have shown in this paper that azimuthally varying chevrons, in particular, the T-fan chevrons can reduce the far field jet noise of isolated nozzles with pylon at typical take-off conditions with high bypass ratio of 7 or so better than the state-of-the-art azimuthally uniform chevron nozzles. The T-fan chevron nozzle by itself reduces low frequency noise without any high frequency lift and, in conjunction with the conventional core chevron nozzle it further reduces the low frequency noise without much increase in HFL. There are also other core AVC nozzles which in conjunction with the T-fan nozzle reduce noise better than the conventional chevron nozzle. The limited source diagnostics reported here corroborates the far field noise characteristics; it also shows that the peak low frequency source for the T-fan nozzle shifts further downstream than the baseline or conventional chevron nozzles – this unique phenomenon needs further scrutiny.

Note that no attempt was made to optimize these AVC nozzles and these are only one design-point comparisons. Hence, it is difficult to generalize the findings to different types of AVCs, but there is hope that we can do even better after some sort of optimization on the AVC geometrical parameters is done from the viewpoints of both acoustics and aerodynamic performance. For practical applications, noise benefits for a nozzle should always be considered along with changes in the aerodynamic performance characteristics, like thrust and discharge coefficients – this has been dealt with for a full-scale flight test of an RT-type nozzle in Nesbitt et al[19] as part of the QTD2 program.

Acknowledgments

References

[1] Janardan, B.A., Hoff, G.E., Barter, J.W., Martens, S., Gliebe, P.R., Mengle, V. and Dalton, W.N., "AST Critical Propulsion and Noise Reduction Technologies for Future Commercial Subsonic Engines – Separate-Flow Exhaust System Noise Reduction Concept Evaluation," NASA/CR-2000-210039, Dec. 2000.

[2] Mengle, V.G., "Relative Clocking of Enhanced Mixing Devices for Jet Noise Benefit," AIAA Paper 2005-0996.

[3] Mengle, V.G., "Jet Noise Characteristics of Chevrons in Internally Mixed Nozzles," AIAA Paper 2005-2934.

[4] Bhat, T.R.S., "Experimental Study of Acoustic Characteristics of Jets from Dual Flow Nozzles." AIAA Paper 2001-2183.

[5] Hunter. C., Thomas, R.H., Abdol-Hamid, K., Pao, S.P., Elmiligui, A.A. and Massey, S.J., "Computational Analysis of the Flow and Acoustic Effects of Jet-Pylon Interaction " AIAA Paper 2005-3083.

[6] Elkoby, R., "Full-Scale Propulsion Airframe Aeroacoustics Investigation," AIAA Paper No. 2005-2807.

[7] Massey, S., Thomas, R., Abdol-Hamid, K. and Elmiligui, A.A., "Computational and Experimental Flow Field Analyses of Separate Flow Chevron Nozzles and Pylon Interaction." AIAA Paper 2003-3212.

[8] Hunter. C., and Thomas, R., "Development of a Jet Noise Prediction Method for Installed Jet Configurations." AIAA Paper 2003-3169.

[9] Thomas, R., and Kinzie, K., "Jet-Pylon Interaction of High Bypass Ratio Separate Flow Nozzle Configurations," AIAA Paper No. 2004-2827.

[10] Mengle, V.G., Elkoby, R., Brusniak, L. and Thomas, R., "Reducing Propulsion Airframe Aeroacoustic Interactions with Uniquely Tailored Chevrons. 2. Installed Nozzles," AIAA Paper No. 2006-2434.

[11] Mengle, V.G., Brusniak, L., Elkoby, R., and Thomas, R. "Reducing Propulsion Airframe Aeroacoustic Interactions with Uniquely Tailored Chevrons. 3. Jet-Flap Interaction," AIAA Paper No. 2006-2435.

[12] Herkes, W.H., Olsen, R. and Uellenberg, S, "The Quiet Technology Demonstrator Program: Flight Validation of Airplane Noise Reduction Concepts," AIAA Paper No. 2006-2720.

[13] Crighton, D.G., "Airframe Noise," in *Aeroacoustics of Flight Vehicles: Theory and practice. Vol. 1: Noise Sources*, edited by Hubbard, H.H., NASA RP-1258, Vol. 1, 1991, Ch. 7, pp. 391-447.

[14] Fink, M.R., "Propulsive Lift Noise," in *Aeroacoustics of Flight Vehicles: Theory and practice. Vol. 1: Noise Sources*, edited by Hubbard, NASA RP-1258, Vol. 1, 1991, Ch. 8, pp. 449-481.

[15] Bridges, J. and Brown, C., "Parametric Testing of Chevrons on Single Flow Hot Jets," AIAA Paper No. 2004-2824.

[16] James R. Underbrink, "Aeroacoustic Phased Array Testing in Low Speed Wind Tunnels", in *Aeroacoustic Measurements*, edited by Thomas J. Mueller, Springer, 2002, Ch. 3, pp. 98-217.

[17] Robert P. Dougherty, "Beamforming In Acoustic Testing", in *Aeroacoustic Measurements*, edited by Thomas J. Mueller, Springer, 2002, Ch. 2, pp. 62-97.

[18] Massey, S., Elmiligui, A., Hunter, C., Thomas, R., Pao, P. and Mengle, V.G., "Computational Analysis of a Chevron Nozzle Uniquely Tailored for Propulsion Airframe Aeroacoustics," AIAA Paper No. 2006-2436.

[19] Nesbitt, E., Mengle, V.G., Czech, M., Callendar, B., and Thomas, R., "Flight Test Results for Uniquely Tailored Propulsion-Airframe Aeroacoustic Chevrons: Community Noise," AIAA Paper No. 2006-2438.